Journal of Adhesion Science and Technology

Publication details, including instructions for authors and subscription information:
http://www.tandfonline.com/loi/tast20

Advanced Icephobic Coatings

Richard Menini [a] & Masoud Farzaneh [b]

[a] NSERC/Hydro-Quebec/UQAC Industrial Chair on Atmospheric Icing of Power Network Equipment (CIGELE) and Canada Research Chair on Engineering of Power Network Atmospheric Icing, Université du Québec à Chicoutimi, Chicoutimi, QC, G7H 2B1, Canada;, Email: rmenini@uqac.ca

[b] NSERC/Hydro-Quebec/UQAC Industrial Chair on Atmospheric Icing of Power Network Equipment (CIGELE) and Canada Research Chair on Engineering of Power Network Atmospheric Icing, Université du Québec à Chicoutimi, Chicoutimi, QC, G7H 2B1, Canada

Published online: 02 Apr 2012.

To cite this article: Richard Menini & Masoud Farzaneh (2011) Advanced Icephobic Coatings, Journal of Adhesion Science and Technology, 25:9, 971-992, DOI: 10.1163/016942410X533372

To link to this article: http://dx.doi.org/10.1163/016942410X533372

VSP

Journal of Adhesion Science and Technology 25 (2011) 971–992

Journal of ADHESION SCIENCE and TECHNOLOGY
brill.nl/jast

Advanced Icephobic Coatings

Richard Menini * **and Masoud Farzaneh**

NSERC/Hydro-Quebec/UQAC Industrial Chair on Atmospheric Icing of Power Network Equipment (CIGELE) and Canada Research Chair on Engineering of Power Network Atmospheric Icing, Université du Québec à Chicoutimi, Chicoutimi, QC, G7H 2B1, Canada

Received in final form 4 November 2008; revised 24 November 2009; accepted 5 September 2010

Abstract

Adhesion and excessive accumulation of atmospheric ice on the surface of exposed objects such as conductors of overhead power lines, cables and conductors in aluminum can have devastating economical and safety consequences as it was the case during the 1998 and 2007 ice storms in Canada and USA. Recent advances in the understanding of ice adhesion on various substrates and in materials science have spurred interest in developing new intrinsic icephobic materials. The aim of this paper is to review the most relevant research activities related to ice adhesion mechanisms and icephobic coating development during the recent years. This will allow a better comprehension of ice adhesion, and help determine more reliable and cost effective ways to develop icephobic coatings, In order to develop icephobic coatings three main groups of materials or surface treatment can be considered: (i) self-assembled monolayers with $-CH_3$ or $-CF_3$ groups oriented outward to the ice surface, (ii) coatings with a heterogeneous chemical composition of at least two highly hydrophobic components to disrupt the structure of the liquid-like layer, and finally (iii) a porous or superhydrophobic deposits to promote the presence of tiny air pockets at the ice/solid interface to disrupt bonding by creating stress concentrations.

Keywords

Icephobic, coatings, SAMs, superhydrophobic

Introduction

Adhesion and accumulation of ice to surfaces may cause major problems on the integrity of outdoor equipment such as telecommunication towers, antennas, power network systems, aircrafts and ships. This could cause tremendous damages sometimes leading to catastrophic socio-economical losses as was the case during the 1998 and 2007 ice storms in Eastern Canada and Oklahoma, respectively. Other icing events, between 1959 and 1994, which were registered in the USA, caused

* To whom correspondence should be addressed. Tel.: 418 545 5011; Fax: 418 545 5032; e-mail: rmenini@uqac.ca

DOI:10.1163/016942410X533372

the collapse of 140 communication towers (40–2000 ft tall) [1]. Also, in the same country, ice accumulation caused the crash of 135 small planes between 1993 and 2004, resulting in 171 casualties [2].

Two main avenues have been explored to combat ice adhesion: (i) active de-icing methods such as thermal and mechanical techniques [3, 4], and (ii) passive methods which do not need external energy for de-icing or preventing ice accretion [3]. Among the latter are included methods based on protecting the exposed surface by applying coatings with icephobic characteristics to significantly reduce or cancel ice adhesion strength. While the first strategy is widely used, the second one should offer more advantages since it is more environmentally friendly when compared to the de-icing fluids used for planes, and cheaper considering the costs involved in device elaboration and operation. Thus, substrate protection with so-called icephobic coatings exhibiting very low ice adhesion strengths looks very promising.

While some commercial hydrophobic coatings are currently labeled 'icephobic', they actually exhibit little benefit over Teflon®, for instance [5, 6]. During the last 15 years, active scientific research has been carried out to develop innovative and cost effective icephobic coatings. A comprehensive review of the accomplished work on ice adhesion would be helpful. In fact, the lack of such a review does not allow one to assess the latest advances and make decisions on the direction for developing reliable and cost effective icephobic coatings. The few literature surveys carried out so far are either specific to one application such as the aeronautics, dam protection or electrical engineering [7–9], or are relatively old [10]. Moreover, none of them bring together all the aspects that can influence adhesion between two solids. Thus, in order to study and to comprehend the best strategies to reduce ice adhesion strength on a given substrate, this paper will focus firstly on the forces acting at the ice–substrate interface as well as on the influences of both ice structure and substrate chemical composition and morphology. Thereafter, a wide range of permanent surface treatments will be reviewed and discussed. It must be pointed out that collateral, but important topics, such as ice adhesion strength measurements in shear mode as well as the different type of atmospheric icing such as rime, glaze, frost as well as wet and dry snow will not be discussed in this paper. However, the reader can find relevant information in the works of Kaasai and Farzaneh [11], Makkonen [12] and Sakamoto [13].

1. Surface Energy

Before studying the ice–substrate adhesion force components, the concept of surface free energy needs to be introduced. Adhesion strength between two materials is referred to as the work of adhesion W_a, which corresponds to the change in free energy when two separated surfaces are created for a given system. The liquid–solid–vapor system is schematically represented in Fig. 1 where γ_{sv}, γ_{lv} and γ_{sl} are the surface energies of the solid, the liquid and the solid–liquid, respectively. The angle Θ is the contact angle between the liquid and vapor phases. The work adhe-

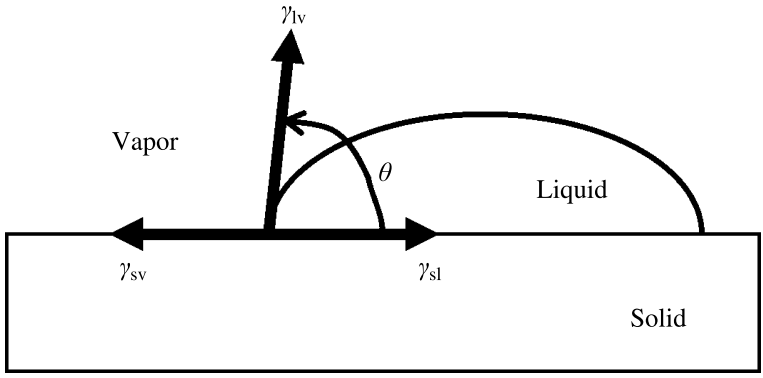

Figure 1. Schematic representation of surface free energies at a triple phase system.

sion is given by equations (1) and (2). It can be seen from equation (2) that the work of adhesion can be derived from contact angle measurements. Young's equation (3) is another way of expressing equation (2).

$$W_A = \gamma_{sv} + \gamma_{lv} - \gamma_{sl}, \tag{1}$$

$$W_A = \gamma_{lv}(1 + \cos\Theta), \tag{2}$$

$$\gamma_{lv}\cos\Theta = \gamma_{sv} - \gamma_{sl}. \tag{3}$$

A detailed description of the contact angle theory of adhesion can be found in references [14–16]. Using equation (2), at contact angle $\Theta = 0°$, adhesion work is $W_A = 2\gamma_{lv}$ and total wetting is observed. If $\Theta = 180°$ then $\cos\Theta = -1$, and W_A becomes zero with no wetting and no adhesion. If $\Theta = 90°$, then $W_A = \gamma_{lv}$, with poor wetting and poor adhesion. Usually, a surface is considered hydrophilic when $\Theta < 90°$. It is said to be hydrophobic when $\Theta > 90°$. It is not straightforward to determine the surface free energy of a given solid γ_{sv} using only Young's equation (3) since γ_{sl} is not known and must be estimated or experimentally evaluated using a Zisman plot ($\gamma_{lv} = f(\Theta)$). In the first relevant work on this topic [17], the total surface free energy was divided in two parts: dispersive and non-dispersive. The first one results from the molecular interaction due to London forces and the second to all the non-London forces. On the other hand, some groups did consider both polar and apolar interactions. Van Oss *et al.* [18] used an acid–base approach to develop their model where the surface free energy is expressed as the sum of a Lifshitz–van der Waals apolar component and a Lewis acid–base polar component. Finally, Zhao *et al.* [19] in their study of the surface free energy of Ni–P–PTFE composite coatings, reviewed and compared three different approaches to determine γ_{sv}. They found some differences but were unable to fully explain them. In the literature, many surface free energy calculations could be found, as seen in Table 1.

Considering the values displayed in Table 1, materials having a surface energy lower than 72 mN m^{-1} should exhibit low ice adhesion strength. PTFE (or Teflon®) and PDMS are among that category and appear to be the best candidates to reduce ice adhesion strength. It must be pointed out that surface energy mea-

Table 1.
Surface free energies for different substrates, from [7, 14, 56]

Material	Surface free surface energy (mN m^{-1})
$-CF_3$ group	6
Poly(tetrafluoroethylene) or PTFE	20
Poly(dimethylsiloxane) or PDMS	22
PVDF	25
Polystyrene	33
Nylon 6,6	46
Copper	60
Liquid water	72
Silica (dehydrated)	78
Anatase (TiO_2)	92
Iron oxide (Fe_2O_3)	107
Aluminum	>100
Steel	>100
Rutile (TiO_2)	143

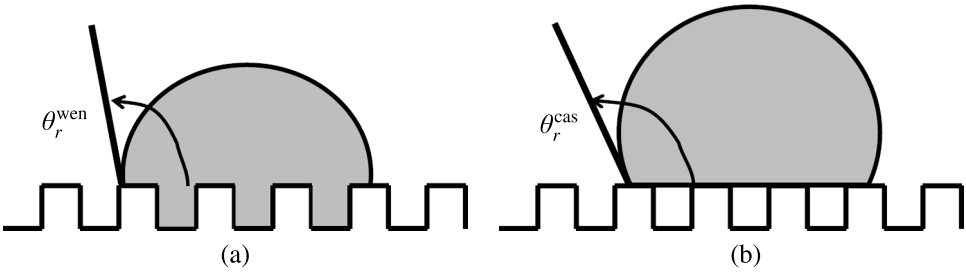

Figure 2. Wenzel (a) and Cassie (b) models for a water droplet deposited on a rough surface.

surements must be performed on ultra clean and very flat surfaces. While the first requirement can be achieved relatively easily, a given material such as an industrial surface has a non-negligible roughness which can influence contact angle measurements. Additionally, very rough surfaces may exhibit a special behavior labeled superhydrophobic or ultrahydrophobic state ($\Theta > 150°$). Several relevant papers and reviews can be found in the literature concerning the theoretical approach of superhydrophobicity [15, 16, 20]. Surface roughness caused by micro- and nano-asperities is usually responsible for the superhydrophobic phenomenon. The value of the contact angle measured on a rough surface corresponds in reality to an apparent contact angle (Θ_r), which is dependant on the roughness as well as on the behavior of the liquid drop at the interface. Two different models were proposed to described this phenomenon: the Wenzel [21] and the Cassie [22] models, displayed in Fig. 2. For both models, equations (4) and (5) give the values of the apparent

contact angles, Θ_r^{wen} and Θ_r^{cas}, in function of the contact angle measured for a flat surface (Θ_{flat}). For the Wenzel model, r is the roughness factor and corresponds to the ratio of the actual area of the rough surface to the projected area. For the Cassie model, φ_s is the area fraction of the solid surface in contact with the liquid.

$$\cos\Theta_r^{\text{wen}} = r\cos\Theta_{\text{flat}}, \tag{4}$$

$$\cos\Theta_r^{\text{cas}} = -1 + \varphi_s(\cos\Theta_{\text{flat}} + 1). \tag{5}$$

Due to their static characteristics, sessile drop contact angle measurements are not sufficient to properly characterize superhydrophobic surfaces, thus two other assessment methods must be used: evaluation of contact angle hysteresis, see equation (6), and evaluation of the sliding angle, see equation (7). Contact angle hysteresis can be evaluated when a liquid droplet attached to a syringe needle is allowed to slide on a given surface. Advancing and receding angles, Θ_{adv} and Θ_{rec}, are measured on the distorted liquid and calculated using equation (6). If $\Delta\Theta \to 0$, the surface has high superhydrophobic properties. As far as the sliding angle technique is concerned, a liquid droplet having known mass and volume is deposited on a given surface placed on a leveled rotating stage. The sliding angle α is the angle that triggers the roll down motion of the droplet. The sliding angle is a function of the mass m of the droplet; the gravitational constant g and the radius of contact area r (see equation (7)). If $\alpha \to 0$, the surface has high superhydrophobic properties. Recently it was discovered that surface having $\Delta\Theta < 5^\circ$ exhibited very high icephobic properties [23, 24]. It must be pointed out that this kind of assessment constitutes only an indication on the icephobic properties of superhydrophibic (or Lotus-type) surfaces since the freezing dynamics are not taken into account. Therefore, it is important to state that the different contact angles measurements for icephobicity assessment are just indicative since they do not play a role in the icing mechanism.

$$\Delta\Theta = \Theta_{\text{adv}} - \Theta_{\text{rec}}, \tag{6}$$

$$\sin\alpha \propto \frac{r}{mg}. \tag{7}$$

2. Ice Adhesion

The binding energies of H_2O molecules to different solids are expected to be similar for water and ice [25]. So, one can assume that the W_a values on different ice–solid interfaces will be correlated with the contact angle of liquid water. In fact, some authors [26–28] measured the shear strength of ice on different materials and compared their results with the corresponding water contact angles. Such results were compiled by Petrenko and Whitworth [25] and are displayed in Fig. 3. The correlation is relatively weak mainly because the surfaces were not smooth and the failure mechanism can differ from one material to another. This correlation seems to follow an exponential trend. However, due to the high scatter in the value, it is difficult to analyze.

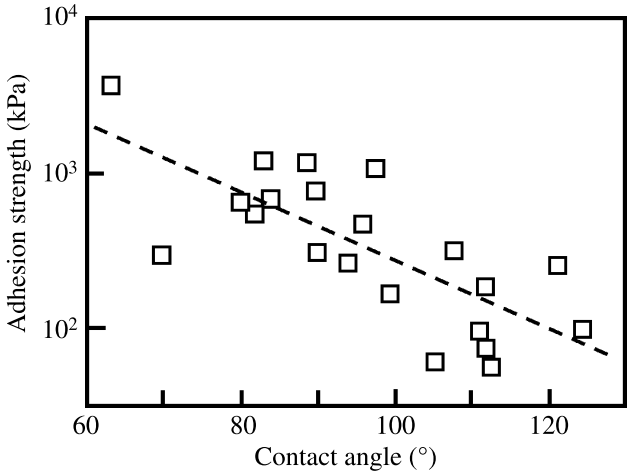

Figure 3. Correlation between the shear strength of adhesion of ice to various plastics and the contact angle, from [25], p. 316.

Adhesion is an extremely important engineering concept, but a complex one to define since different types of adhesion forces or intermolecular forces may be present. At the atomic or molecular levels, short range (0.15–0.3 nm) interactions forces are present such as covalent, electrostatic, and/or metallic forces. Long range interactions (>0.3 nm) correspond to the so-called attractive van der Waals forces. Mechanical adhesion may also occur due to mechanical interlocking of microscopic asperities at the interface between two materials [14]. Another factor influencing adhesion is diffusion, but it does not play a role in the case of ice adhesion to common engineering substrates. In fact, it is highly improbable that water molecules diffuse into metals, ceramics or polymers. Usually it is well accepted that ice–materials interactions is a combination of the following four parameters:

- Electrostatic forces,
- Hydrogen bonding,
- van der Waals forces,
- Mechanical adhesion.

Additionally, the presence and structure of a liquid-like layer (LLL) at the ice–substrate interface influences greatly the adhesion strength. Furthermore, depending of the chemical composition of the solid and the type of precipitation, the microstructure of ice can vary enormously.

Electrostatic Forces

Electrostatic interactions occur between adhesive materials and substrates when they have different electronic band structures [11], and when both materials gain charge through an imbalance of charges. Electrostatic attraction theory is based on Coulomb's law and acceptor–donor interactions. Petrenko and Ryzhkin [29–31] theoretically studied in depth the electrostatic interaction taking place at ice/metal

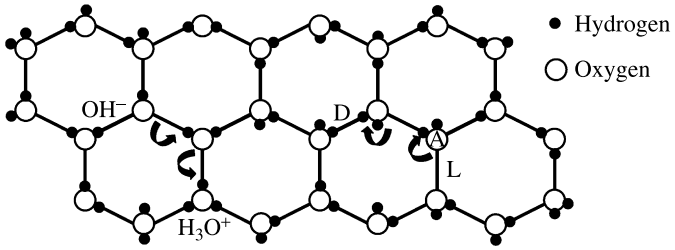

Figure 4. Ionic and Bjerrum defects in the ice structure, from [25], p. 74.

or ice/dielectric materials. Their theory is based on the Jacard theory [31] that states that electrical charge in ice is transferred by protonic point defects: L, D, H_3O^+ and OH^-, as shown in Fig. 4, which play a role similar to electrons and holes in electronic semiconductors. The empty bond is an L-defect and the bond with two protons is a D-defect (doubly occupied). The other two defects correspond to ionic defects resulting from the water ionization reaction:

$$2H_2O \leftrightarrow H_3O^+ + OH^-. \tag{8}$$

At an ice crystal surface, some of the protonic defects may be captured in the surface states, which have energies lower than those in the bulk of the ice. The capture of charged protonic defects in the surface states will result in a surface charge build-up, and therefore in the creation of a surface electric field. Additionally, at a metal or dielectric surface, a surface charge is also created and due to this double layer structure an electrostatic attraction takes place. The corresponding force, or image force, is described by equation (9) [31] where the solid has an effective dielectric constant (ε) larger than that of ice (ε_{ice}). This equation shows that image force F is inversely proportional to the square of the distance to the interface r, where q is the charge and ε_0 the absolute permittivity in vacuum.

$$F = \frac{q^2}{16\pi\varepsilon_0\varepsilon r^2}\frac{\varepsilon_{ice} - \varepsilon}{\varepsilon_{ice} + \varepsilon}. \tag{9}$$

Considering the energies of these different defects, Petrenko and Ryzhkin [30] theoretically evaluated the adhesive energies for an ice/metal interface as a value between 1.3 and 0.08 J m^{-2}. These values were comparable or even higher than those experimentally found at −20°C. Petrenko *et al.* [30] assumed that the very same mechanism is applicable to the ice/insulator interface, and comparisons were made with other studies in the literature. A charge q_{ice} on the ice surface induces the 'image charge' in a metal, while the very same charge q_{ice} will induce a smaller 'image' charge q_{diel} in the insulator, where ε_{diel} is the dielectric permittivity of the insulator, as shown in equation (10). In most solid dielectrics, ε_{diel} is much higher than 1 and the induced charges are comparable with ones induced in metals. The

lower the value of ε, the lower is the electrostatic-related adhesion. For instance, Teflon® has a very low ε ($\approx$2.1) and exhibits icephobic properties.

$$q_{\text{diel}} = q_{\text{ice}} \left(\frac{\varepsilon_{\text{diel}} - 1}{\varepsilon_{\text{diel}} + 1} \right). \tag{10}$$

Lifshitz–van der Waals Forces and Hydrogen Bonding

The Lifshitz–van der Waals interaction forces are always present. It is the most common among interfacial forces, and is considered as a universal interaction resulting from a temporary dipole–dipole interactions. The Lifshitz–van der Waals interaction between ice and several metals and insulators was calculated by Wilen *et al*. [32]. They concluded that this mechanism is not the dominant factor in the case of ice adhesion. This was confirmed by van Oss *et al.* [18], who found that the Lifshitz–van der Waals non-polar component to the ice surface tension was less than that of the polar Lewis acid–base component. Van Oss *et al.* [18] measured the contact angles of a flat, polycrystalline ice surface with a number of liquids. They concluded that the contribution of the Lifshitz–van der Waals non-polar component to the ice surface tension (26.9 mJ m^{-2}) was less than that of the polar Lewis acid–base component (39.6 mJ m^{-2}) which, in the case of ice, is due to hydrogen bonding. Chemical bonding between ice and other solids is considered to be largely hydrogen bonding but this has not yet been studied in detail [33].

Influence of Surface Roughness

Functionalized surfaces are never perfectly plane. Ceramic insulators and alloys of aluminum and stainless steel exhibit a certain surface roughness or even porosity. Before solidifying, water may penetrate the 3-dimensionnal surface structure which could result in the creation of strong joints and mechanical interlocking. A comprehensive review of the ice adhesion due mechanical interlocking can be found in [11]. The expansion coefficient of water around 0°C is greater than that of metals and oxides. Water expands upon freezing, whereas metals and the oxides contract. On the other hand, if a top-down freezing process takes place at a porous surface, air may be entrapped in some pores and the resulting pressure build-up can be significant and may lead to crack initiation and propagation as well as ice de-bonding [34]. The pressure generated within such a surface is actually an internal or residual stress, a condition well known to structural engineers. Therefore, pressure buildup, or residual stress, can be used for ice de-bonding, a topic that will be covered in the next section.

Liquid-Like Layer

It is well known that surface properties are different from those encountered in bulk material. This is seen in the formation of a liquid like layer (LLL) at the different interfaces of a given solid below its bulk melting point (T_{m}). The reader will find valuable information on the theory and experimental ways to study the LLL of ice in the following references [32, 35–42]. The lower the temperature the thinner

is the LLL. In our everyday life, LLL plays an important role in ice adhesion, as ice is usually close to its melting point. In deed in this respect ice is one of the rarest materials we come across. From an experimental point of view, the thickness of the LLL varies from few nm to hundreds of nm depending on temperature and substrate nature. However, as pointed out by Daikhin and Tsionsky [35], a wide range of thicknesses may exist for a given temperature and this is due to the substrate or the gas phase nature. From a theoretical point of view, authors studied the LLL from different approaches: influence of the dipole moments [43], electrostatic charge [44], van der Waals interactions [32], using thermodynamic activity [45] or the hydration forces theory [35]. Only the last two groups showed that the LLL thickness close to the bulk melting point was close to the experimental values (tens of nm). The other works calculated thickness ranging from 1 to 5 nm. From an application point of view, the LLL plays an important role in ice adhesion strength since the liquid layer has a similar behavior to a wetting substance between the two surfaces (ice and solid), hence increasing the effective contact area between them and affecting ice adhesion. As far as the structure of LLL is concerned, water molecules are substantially oriented in the same direction. Thus, the hydrogen atoms (positive charges) either face outward or inward creating an electrical double layer like those commonly encountered in liquid–solid interfaces. Petrenko *et al.* [4, 46–49] used both the semi-conductive properties of ice and the LLL to selectively modify the ice adhesion strength between ice and other surfaces by applying a potential difference between the ice and the solid.

Ice Micro Structure

The coating microstructure, immediately adjacent to a substrate, is very important for the materials engineer. In the case of ice, the interface microstructure at a metallic or metal oxides surface usually range from large polygonal crystals or grains to smaller ones with the same shape produced by recrystallization. The overall process occurs within a few hours after initial freezing [26, 27, 50]. This process leads to the accumulation of dislocations at the ice surface and occurs in any polycrystalline material subject to a steady stress. The latter occurs due to differences in the thermal coefficients of expansion and contraction between the ice and the solid. There are also volume changes as ice forms and cools [27]. As a rule of thumb, the greater the grain size, the lower is the ice adhesion. Druez *et al.* [50] studied the microstructure of droplets of impacted ice on aluminum conductors and showed that the adhesion strength decreased with increasing ice grain size, which in turn was dependent on temperature and air velocity inside the wind tunnel. In fact, ice grain size decreases as wind velocity increases. Ice grain size also decreases as temperature decreases. Penn and Meyerson [34] found that the ice crystals (or grains) not directly attached onto steel, cement concrete, asphalt concrete and glass substrates are randomly oriented polygons, and that the crystals directly attached to substrate surfaces are much smaller polygons (or needles, in the case of steel) and free of air bubbles. The layer formed by these crystals can be assumed to be stronger than the bulk ice because of

the small size of the crystals and the absence of visible flaws. The presence of such a layer would explain the high adhesion strength of ice on this type of material. It would also suggest that the adhesion of ice to any substrate is a severe problem, and that ice removal procedures are likely to leave a thin layer of adhered ice behind. They also studied the appearance of ice crystals on polystyrene and found that the ice interference fringes on this material were significant. Interference fringes are an indication of mechanical stress within the ice crystals themselves. Stress is due to the low thermal conductivity and high coefficient of thermal expansion of polystyrene.

3. Materials for Ice Adhesion Prevention

Linking experimental results to the corresponding theoretical development is an arduous task in the case of ice–solid interfaces. Firstly, on the ice side, many types of ice are encountered in nature: wet and dry snow, rime and glaze. Contaminants and air bubbles may be also present. Secondly, on the materials side and from an engineering point of view, no atomically clean or flat surface exists, and as a result experimental results on adhesion are very difficult to compare with theory. Nevertheless, it seems evident that chemical, electrostatic and mechanical interactions between the substrate and ice, and the properties of the LLL are the main factors affecting the adhesion strength of ice. Consequently, one must focus on these two factors to develop new icephobic coatings. Substrate roughness also plays a crucial, though complex role in ice adhesion strength: while strong mechanical interlocking may occur, ice cracking and in some instances ice de-bonding can be observed due excessive pressure build-up resulting from air trapped in closed pores. Therefore, the engineering of an optimum surface roughness, having superhydrophobic properties for instance, may create enough internal stress to de-bond ice. Mulherin and Haehnel [6] summarized the main criteria in an attempt to develop icephobic materials:

(i) capacity to significantly reduce ice adhesion strength,
(ii) durability or longevity,
(iii) cost effectiveness,
(iv) ease of application.

While the first criterion will always be the most important and obvious one, the other three can be ranked in a different order of importance depending on the application. To illustrate this relative importance, let us consider criterion (ii) and compare the following case. Among the different debris that impinge upon NASA's space shuttle launches, ice coming off from feedline brackets represents a considerable hazard [51]. In this particular situation, the longevity of an icephobic coating would not be an issue since the latter should keep its properties only during the pre-launching and launching stages. On the other hand, icephobic materials to be coated on high voltage power lines must remain active for forty five years or so. During this time, the coated material must withstand several electrical, mechanical,

and thermal constraints generated during the normal operating conditions or during specific defaults such like a short-circuit or a lightning strike [9]. Generally, usual coating properties common to each specific application must be taken in account by the engineer when developing a new coating. These correspond to material degradation mainly due to corrosion, wear, erosion, UV illumination and a combination of them.

It should be noticed that in the references cited hereafter, ice adhesion strength values were measured in shear mode. However, to avoid misleading data comparison between different authors, no adhesion strength values will be given. In reality, any comparison is shaky since the measurement apparatus were not always the same, ice deposition processes usually differed, and coating roughness were not constant from one author to the other. Three types of coatings may be used to prevent ice accumulation on structures:

- very low surface energy coatings,
- heterogeneous/composite coatings,
- porous/superhydrophobic coatings.

Low Surface Energy Coatings

Deposition of a material having the lowest surface energy possible is the main objective in finding suitable icephobic coatings. According to Table 1, poly(dimethylsiloxane) (PDMS or silicone), Teflon® and poly(tetrafluoroethylene) (PTFE) are the best candidates, see Fig. 5. Numerous researchers have elaborated and tested coatings based on these two families of polymers [5, 6, 26, 27, 52–63]. The reader will also find valuable information in the review by Frankenstein [8]. Coating deposition techniques are usually very simple and involve paints (alkyd or acrylic) with special solvents [27] or the use of polymer resins [54, 63]. Overall, silicone-based polymers are found to perform slightly better than the PTFE-based ones.

As far as PDMS is concerned, Jellinek *et al*. [56] found that a PDMS film had a surface tension of 21 mN m^{-1}, which is characteristic of the methyl groups lying just at the surface of the polymer film, as displayed in Fig. 6. Moreover, these authors show that the dimethylsiloxane content ($-O_2Si(CH_3)_2$ groups) must lie in a certain range of weight percentage and chain length, and that the glass transition temperature T_g must remain low. The T_g temperature corresponds to a measure of molecular segment mobility. When a polymer has a low T_g, and the segments can change places by actively sliding or jumping, the polymer is said to be flexible or

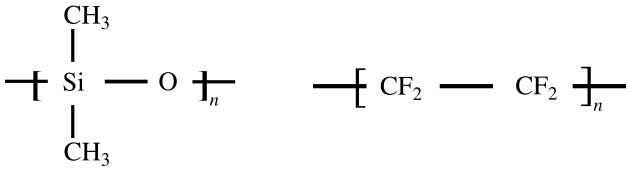

Figure 5. Polysiloxane (a) and polytetrafluoroethylene (b) structures.

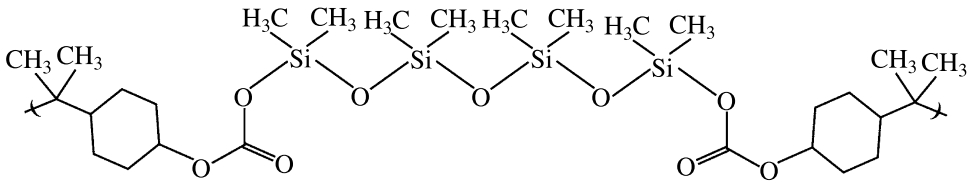

Figure 6. Siloxane-carbonate block polymer, from [56].

soft and correspond to an amorphous state. Ice adhesion can be lowered by the addition of silicone oil which enhances the softness of the PDMS surface by acting as a lubricant and a plasticizer. Anderson *et al*. [64] also showed that low T_g polymers exhibited low interfacial shear strength, but remained constant for $T_g < -50°C$. To summarize, the dissimilar rheological–mechanical properties between ice and polysiloxane-based polymers results in very low ice adhesion. That does not mean that this dissimilarity is necessary to achieve high hydrophobicity, and the polyfluorocarbon (PFC)-based polymers are a good examples. For PFC, the $–CF_2$ and $–CF_3$ groups exhibit low critical surface tension but can have high T_g values ($>150°C$). For the $–CF_3$ group alone, the surface tension was estimated to be 6 mN m^{-1} which is exceptionally low considering the other data displayed in Table 1 [56]. PFC-based materials exhibited better adhesion (on the substrate to be protected) and better mechanical properties (in wear for instance) than its PDMS counterpart. Therefore, for temporary applications, PDMS-based coatings would be a preferable option. It is somewhat peculiar that PTFE, having a strong hydrogen type of bonding with water molecules as well as a high T_g value, is one the most hydrophobic and icephobic substances. However, as seen in the first section, the very low permittivity of PTFE reduces drastically the most important force involved in ice adhesion: the electrostatic force.

Two recent comparative studies were published in order to assess the potential icephobic properties of different commercially available coatings. In the first one, Mulherin and Haehnel [6] tested 16 commercial materials labeled ‘icephobic’, and concluded that these products reduced the amount of energy needed to remove ice but did not prevent ice build-up. The most interesting fact is that all these materials offered very little benefit over Teflon® and even polyethylene (UHMV) cladding. In the other study, ice adhesion tests using a centrifuge test apparatus on permanent and non-permanent coatings [5] showed that there is no perfect icephobic material based on the criterion that the ice can detach itself from the icephobic surface under its own weight or under the action of wind. As far as permanent coatings are concerned, the results show that one of the best commercially available materials, Wearlon®, provides an ice reduction adhesion of only 12 compared to the non-permanent coatings, which is also less than twice the reduction factor obtained for PTFE. According to its manufacturer [65], the Wearlon® chemistry involves grafted silicone molecules onto epoxy molecules, thereby distributing the silicone throughout the epoxy matrix. For non-permanent coatings, the best results were ob-

tained with lithium grease and industrial lubricants with a reduction factor of about 63 compare to bare aluminum, which both provide a thin viscous or liquid film between the ice and the substrate. However, these viscous icephobic materials are not well adapted for some application such as electrical network conductor and ground cables because they require recurrent applications due to their non-permanent nature [66].

By preventing the freezing of supercooled water droplets impacting on surfaces, other types of non-permanent coatings aim at keeping a thin water film between the surface and the ice thus facilitating natural ice shedding by gravity. Creating a water film between ice and the substrate can be simply achieved by using liquids which decreases the freezing point of water when mixed with the latter. These commercially available products are commonly used to protect aircraft and pavement from ground icing. However, like the other viscous icephobic materials described above, they present the same constraints of applicability and duration [67], requiring timely and recurrent applications to provide effective ice protection. In that context, they should be used punctually for specific and strategic needs. Overall, these studies show that development of new advanced permanent icephobic materials is needed to surpass PTFE or PDMS as well as the non-permanent coatings.

As pointed out by Croutch *et al*. [27], in order to obtain maximum water repellency, $-CH_3$ and $-CF_3$ groups must be oriented outward from the coating surface. An attractive technique to obtain such oriented layers is to deposit self-assembled monolayers or SAMs. SAMs are molecular assemblies that are formed spontaneously by the immersion of an appropriate substrate into a solution of an active surfactant in an organic solvent, as shown in Fig. 7. In this figure, an organosilicon type of anchoring group was chosen to illustrate this deposition technique since this group covalently binds to several important metal or non-metal oxides such as

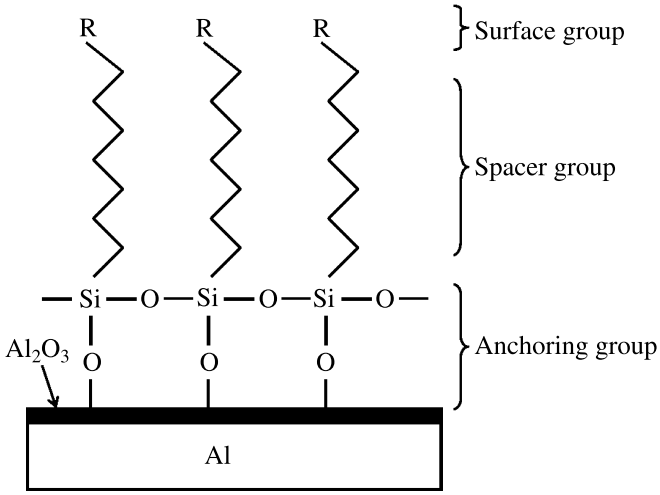

Figure 7. Schematic representation of SAMs grafted onto an aluminum substrate.

Al_2O_3, TiO_2, SnO_2, SiO_2, glass, etc. The spacer group consists of an alkyl chain while the surface group can be chosen accordingly to the desired surface property. For icephobicity, $\mathbf{R} = -CF_3$ and $-CH_3$ are obvious candidates.

Another advantages of SAMs is that the covalent nature of the bonding makes the anchoring of the alkyl chain very strong and that the overall deposition technique is easy to implement and inexpensive. Somlo and Gupta [68] have shown that ice adhesion decreases when a SAM of dimethyl-n-octadecilchlorosilane is formed on an Al alloy surface. More recently, Petrenko and Peng [33] have applied mixtures of self-assembling 1-dodecanethiol and 11-hydroxylundecane-1-thiol with various degrees of hydrophobicity/hydrophilicity on Au surfaces and have shown a good correlation between the contact angle of water and the ice adhesion strength. Kemmell *et al*. [69] produced nanostructured superhydrophobic surfaces prepared by the self-assembly of hydrophobic n-octadecyltrimethoxysilane ($H_3C(CH_2)_{17}Si(OCH_3)_3$) and (3,3,3-trifluoropropyl)trimethoxysilane ($F_3C(CH_2)_2Si(OCH_3)_3$) monolayers from gas phase on porous alumina, ZnO nanowire and GLAD (glancing angle deposition) surfaces. Nevertheless, as pointed out by Kulinich and Farzaneh [70] there is still a lack of systematic knowledge on how the microstructure and surface chemistry of SAMs influence their hydrophobic and icephobic properties. In fact, the case depicted in Fig. 7 is an ideal one: the surface is perfectly plane and all the surface active groups are ideally positioned. In the presence of a porous or rough surface, chains of molecules get bent or collapse, resulting in a hydrophobicity decrease due to surface exposing of alkyl groups such as $-CF_2$ or $-CH_2$ [70, 71].

Another aspect to be explored is based on the fact that coating efficiency is related only to one or two layers of molecular chains. In other words, if some patches of the substrate to be protected get damaged, the risk of increase ice adhesion is high. However, this technique represents a very attractive strategy to reduce ice adhesion. Researchers have to develop robust SAMs with good ageing properties that remain active whatever the surface topography is.

Plasma Enhanced Chemical Vapor Deposition (PECVD) can produce diamond-like coatings (DLC) through the ionization and radicalization of a feeding gas that can be C_2F_6 [72]. Highly reactive radical species such as $CF_2^{\bullet}$ or $CF_3^{\bullet}$ are produced during the PECVD process and are subsequently deposited on the desired surface forming a dense, hard and highly adhesive coating and therefore having high life expectancy. Recent studies have demonstrated the potential of ultra thin films based on DLC associated with a fluorocarbon gas [72–76]. These coatings produced by common PECVD technology, exhibit high hydrophobicity with high adhesion to aluminum and porcelain, and good mechanical properties. This technique may also be used to coat micro-textured surfaces to make them superhydrophobic. Although, coatings with very good mechanical properties can be made with the PECVD technique, several issues or limitations must be considered: high cost; the low thickness of the films (around 1 μm) as well as the difficulty to plate large and complex-shaped substrates with this non-line-of-sight technique.

Heterogeneous and Composite Coatings

Croutch *et al*. [27], Hacker *et al*. [54] and Reich [62] found that by mixing polysiloxane and fluorocarbon type of materials they can lower ice adhesion more than homogeneous coatings with either PDMS or the PFC types of structure alone. However, these authors did not explain why this kind of heterogeneity leads to significant lower ice adhesion strengths. In 1994 and 1997, Murase *et al.* [77, 78] published two papers on heterogeneous polymer coatings aimed at decreasing ice adhesion. These authors studied three different types of heterogeneous polymer: organopolysiloxane grafted with fluoro polymer (A), polyperfluoroalkyl(meth)acrylate combined with hydrophobic silicon dioxide (B), and an organopolysiloxane modified with a lithium compound ($LiMO_3$) (C). Snow accretion was not possible on the (B) coating while ice adhesion was reduced two fold compared to PTFE. On the other hand, ice adhesion was 25 times lower for compound (C) compared to PTFE; at the same time, however, snow accretion was only reduced by a factor of two. To explain such a decrease in ice or snow adhesion in the presence of a heterogeneous polymer (block-co-polymers), Murase performed molecular orbital energies calculations using the SCF method with the MOPAC program. Three molecules were analyzed: ethane (C_2H_6), dimethylesiloxane (DMS) and hexafluoroethane (C_2F_6). The hydrogen bond lengths (O–H and F–H) as well as the different interaction energies were evaluated. These authors found that hydrogen bonds energies and lengths were very different depending on the kind of molecular group involved. In reality, there was a slight repulsion between a water molecule and a siloxane group, while a strong attraction was calculated for the fluorocarbon group and a H_2O molecule. It is worth mentioning also that the water molecule orientation at the surface of the fluorocarbon group and at the polysiloxane one was completely different. Therefore, by creating at the molecular level various disparities in term of energy bonding and water molecule orientation, the ice–material interface is weakened with the probable creation of a wide range of dislocations and slips in the structure of the LLL. A patent by Byrd [79] from the Boeing company described the elaboration of a polysiloxane(amide-ureide) coating for icephobicity applications. The idea is the same as the one described by the Murase group: the heterogeneity of this polymer creates a synergistic effect which leads to low ice adhesion strength. In another patent, Mizuno *et al*. [80] developed a heterogenous coating using a tetrafluoroethylene and a silicone resin with an appropriate organic solvent.

Hydrophobic composite coatings were also prepared using electrodeposition and electroless plating where micro or nano-PTFE particles are dispersed in a given electrolyte and get entrapped during the reducing process of the metallic ions. Using an electroless technique, Der Ger *et al*. [81] have produced Ni–P–PTFE coatings exhibiting a water contact angle of 110°. Zhao *et al*. [19] also found similar results with the same technique. Ultra-dispersed nano-sized (300 nm) PTFE particles within a nickel matrix were produced by Wang *et al*. [82] using electrodeposition. They measured water contact angles ranging from 123° (28% vol. inclusion of

particles) to 155° (47% of particles). However, no studies about ice adhesion on electrocomposite coatings can be found in the literature. Therefore, it would be very interesting to assess the icephobicity of this kind of material. Even though the presence of a high surface energy area (metal) may be problematic, the composite nature of the surface may lead to interesting new properties. Electrochemical deposition techniques are very cheap, and can produce thick adhesive films (between 1 and 100 μm). Additionally, large and complex parts can be plated.

Superhydrophobic and Porous Materials

Surface roughness can have a spectacular influence on hydrophobicity. Numerous examples can be found in nature where the surfaces of some plants [83–85] or animals [86–88] exhibit superhydrophobic behavior. In such instances, water drops tend to behave like pearls and can roll down from those surfaces. This phenomenon allows some plants or animals to remove dirt from their surface by collecting them through the water drop motion and fall. To mimic nature, numerous superhydrophobic (SH) materials have been developed [89] but few of them were intended for icephobic applications. A first strategy to obtain SH materials is to create a primary porous structure by either etching a given substrate [90], depositing oxides nanoparticles [91] ZnO 'nano-towers' [92], using nanolithography [93] or by electroplating polymers [94, 95]. Lau *et al*. produced a carbon nanotube forest using the PECVD technique. The given material was subsequently coated with PTFE to obtain superhydrophobicity [96]. In a second step, a low surface energy thin film was deposited on the 3-D structure using various techniques such as PECVD, deposition of SAMs [69, 71] and passivation with stearic acid [92], as shown in Fig. 8. SH structure can also be made of hydrophobic molecules such as micro- or nano-fibers. Zhang *et al*. [97] made PTFE a superhydrophobic surface by extension of the fibers comprising the base material. Feng *et al*. [98] produced a superhydrophobic poly(vinyl

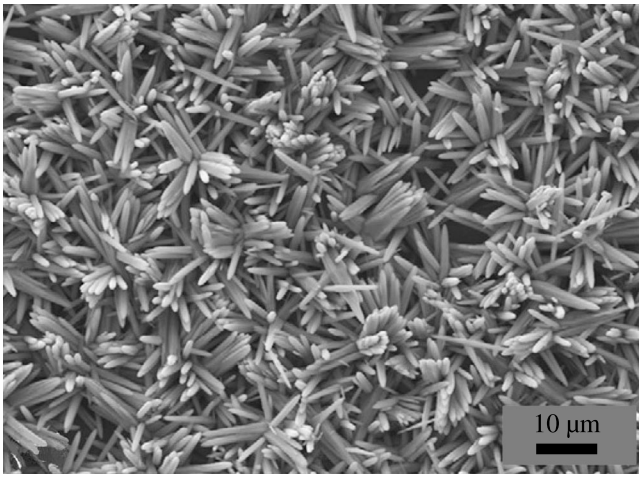

Figure 8. SEM image of ZnO nanotowers [92].

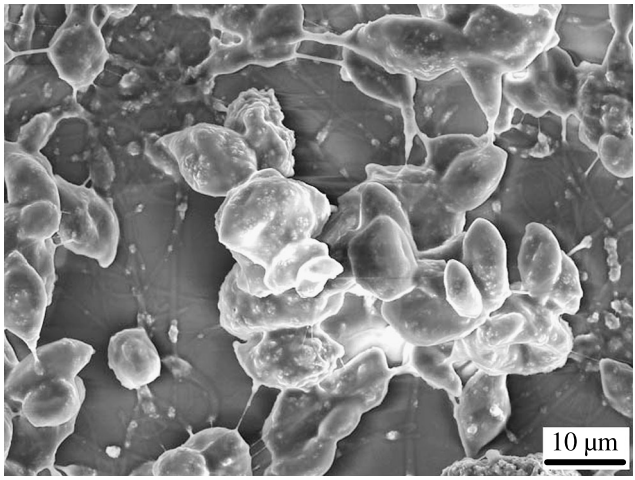

Figure 9. SEM image of electrospun poly(tetrafluoroethylene-*co*-vinylidene fluoride-*co*-propylene) fibers [101].

alcohol) forest-like nanofiber structure by extruding the polymer through an alumina template with holes of diameters ranging between 20 and 500 nm. Production of nano-fiber networks using the electrospinning process has also recently drawn some attention. Poly(caprolactone) was electrospun and then coated with a thin layer of hydrophobic polymerized perfluoroalkyl ethyl methacrylate (PPFEMA) by iCVD [99]. Other superhydrophobic electrospun fibers are poly(AN-co-TMI) with a perfluorinated linear diol (fluorolink-D) and tin(II) ethyl hexanoate in DMF [100] and polymer (PFC) fibers with embedded nanoparticles [101], as shown in Fig. 9. In each of these studies, superhydrophobicity was achieved when the structure of the materials was composed of both fibers and polymer beads. It must be pointed out that for all the above-mentioned superhydrophobic coatings, none of them was tested under icing conditions. The work of the Saito group in Japan [102–106] developed highly hydrophobic micro-textured coatings made of PTFE particles blended in a PVDF ($-(CH_2-CF_2)_n-$) binder applied by a spray drying technique. Snow accretion on antennae was dramatically reduced by such coatings. However, the most important advances in superhydrophobic coatings having icephobic properties were developed by the Farzaneh group [24, 107–109]. Different oxidized aluminum substrates were etched and subsequently coated with metal oxide compounds which in turn were coated with RF-sputtered Teflon. This type of coatings exhibited tremendous reduction of ice adhesion strength.

In 2003, He *et al*. [110] verified experimentally that both Wenzel and Cassie models described in Fig. 2 depended on the water drop deposition process. A gentle droplet deposition resulted in a Cassie-type regime while a droplet dropped from a certain height resulted in a Wenzel-type one. These experimental results are crucial if one wants to consider micro-textured materials for icephobic applications since supercooled water droplet impacts may result in liquid inclusion and its subsequent

and rapid freezing inside the 3-D structure. Because of the unique expansion property of ice at the freezing point, the ice formed in blind pores would push tight against the walls, resulting in strong mechanical interlocking. On the other hand, Penn and Meyerson [34] who studied various aspects of icing on porous pavements, measured a pressure rise during freezing inside an enclosed space. However, if air is entrapped the pressure build-up can be significant and can lead to crack initiation and propagation as well as ice de-bonding. These authors measured the pressure rise during freezing as a function of the initial volume of water trapped in an enclosed space. When 2% of the water was frozen the pressure was 36 atm and for 20% of ice formed the pressure reached 420 atm. The pressure generated within the specimen is actually internal or residual stress. To use the pressure, or residual stress, to their advantage (ice de-bonding), they drilled holes into a pavement portion, performed top-down freezing, and depending of the size of the holes the ice caps popped up after a certain time. In another work from Bascom *et al.* [26], replicas of the ice sheared from four different PDMS coatings showed bubble-like features that strongly suggested that tiny air bubbles had been trapped between the ice and the coating resulting in low ice adhesion properties. Development of new materials having an optimum roughness in order to create enough internal stress to crack and hopefully de-bond ice, is promising.

4. Conclusion

Merely testing commercial hydrophobic coatings hoping that they have some kind of icephobic properties is something of the past. New pressures call for innovative advanced coatings to drastically reduce ice adhesion strength. Recent advances in ice adhesion physics and materials science have spurred new interest in developing new intrinsic icephobic materials or coatings able to perform better than PTFE for instance. To decrease ice adhesion on a given solid, its surface has to be modified or coated with a material capable, at the molecular or crystal level, of disrupting the structure of the ice immediately adjacent to the solid. Several strategies can be exploited to achieve such a goal, and the best materials will belong to one or several of the following three families:

- Coatings having $–CH_3$ or $–CF_3$ groups closely packed at material surface such as in SAMs.
- Materials with an heterogeneous surface chemical composition with at least two highly hydrophobic component to disrupt the structure of the LLL.
- Superhydrophobic or porous coatings to promote the presence of tiny air pockets at the ice/solid interface in order to reduce the real ice/coating surface area and disrupt bonding by creating stress concentrations.

Future directions to improve icephobicity of such materials must focus firstly on establishing the relative influence of the electrostatic forces *versus* the forces due to hydrogen bonding for the interaction between the substrate and the ice. Secondly, concerning coating surface morphology, the influence on icephobicity has

to be studied in conditions close to real precipitations. For instance, the behavior of supercooled water droplets having different size and velocities impinging on the treated surfaces must be studied.

Finally and from the engineer point of view, material's durability or longevity, its cost and ease of application are also major items to consider but are specific to the application. Excellent coating adhesion to the substrate, resistance to ageing due to corrosion (normal or accelerated by acid rain or the nearby presence of seawater), UV illumination, thermal exposure, and wear (during installation of high voltage lines for instance), as well as to erosion/abrasion due to the combined effects of rain and wind are among the most important factors to take into account.

Acknowledgements

This work was carried out within the framework of the NSERC/Hydro-Quebec/UQAC Industrial Chair on Atmospheric Icing of Power Network Equipment (CIGELE) and the Canada Research Chair on Engineering of Power Network Atmospheric Icing (INGIVRE) at Université du Québec à Chicoutimi. The authors would like to thank the CIGELE partners (Hydro-Québec, Hydro One, Réseau Transport d'Électricité (RTE) and Électricité de France (EDF), Alcan Cable, K-Line Insulators, Tyco Electronics, CQRDA and FUQAC) whose financial support made this research possible.

References

1. N. D. Mulherin, in: *Proc. of the International Workshop on Atmospheric Icing of Structures, IWAIS'96*, Chicoutimi (QC) Canada, June 3–6 (1996).
2. A. Imse, *The Denver (CO) Rocky Mountain News*, January 24 (2005).
3. M. Farzaneh, C. Volat and A. Leblond, in: *Atmospheric Icing of Power Networks*, M. Farzaneh (Ed.), Chapter 6. Springer (2008).
4. V. F. Petrenko, M. Higa, M. Starostin and L. Deresh, in: *Proc. of the Proceedings of the International Offshore and Polar Engineering Conference*, Honolulu, Hawaii, USA, May 25–30 (2003).
5. C. Laforte and A. Beisswenger, in: *Proc. of 11th International Workshop on Atmospheric Icing of Structures, IWAIS*, Montréal (QC) Canada, June 12–16 (2005).
6. N. D. Mulherin and R. B. Haehnel, Ice Engineering Technical Note 03-4 (October 2003).
7. Y. Boluk, Report, TP 12860E, Optima Specialty Chemicals and Technology Inc. November (1996).
8. S. Frankenstein and A. M. Tuthill, *J. Cold Reg. Eng.* **16**, 83 (2002).
9. C. Volat, M. Farzaneh and A. Leblond, in: *Proc. of the 10th International Workshop on Atmospheric Icing of Structures*, Montréal (QC), Canada, June 12–16 (2005).
10. J. Sayward, Report, U.S. Army Cold Regions Reserach and Engineering Laboratory, Hanover, NH, USA (1979).
11. M. R. Kasaai and M. Farzaneh, in: *Proc. of the International Conference on Offshore Mechanics and Arctic Engineering — OMAE*, Vancouver (BC), Canada, June (2004).
12. L. Makkonen, *Phil. Trans. R. Soc. Lond. A* **358**, 2913 (2000).

13. Y. Sakamoto, *Phil. Trans. R. Soc. Lond. A* **358**, 2941 (2000).
14. D. Myers, in: *Surfaces, Interfaces, and Colloids: Principles and Applications*, 2nd edn. Wiley-VCH, New York, Toronto (1999).
15. D. Quéré, *Physica A* **313**, 32 (2002).
16. D. Quéré, *Rep. Prog. Phys.* **68**, 2495 (2005).
17. F. M. Fowkes, *J. Phys. Chem. B* **66**, 382 (1962).
18. C. J. Van Oss, R. F. Giese, R. Wentzek, J. Norris and J. Chuvilin, *J. Adhes. Sci. Technol.* **6**, 503 (1992).
19. Q. Zhao, Y. Liu and E. W. Abel, *Appl. Surf. Sci.* **240**, 441 (2005).
20. J. Bico, U. Thiele and D. Quére, *Colloids Surf. A* **206**, 41 (2002).
21. R. N. Wenzel, *Ind. Eng. Chem.* **28**, 988 (1936).
22. A. B. D. Cassie and S. Baxter, *Trans. Faraday Soc.* **40**, 546 (1944).
23. S. A. Kulinich and M. Farzaneh, *Langmuir* **25**, 8854 (2009).
24. D. K. Sarkar and M. Farzaneh, *J. Adhes. Sci. Technol.* **23**, 1215 (2009).
25. V. F. Petrenko and R. W. Whitworth, in: *Physics of Ice*. Oxford University Press, Oxford, New York (1999).
26. W. D. Bascom, R. L. Cottington and C. R. Singleterry, *J. Adhes*. **1**, 246 (1969).
27. V. K. Croutch and R. A. Hartley, *J. Coat. Technol.* **64**, 41 (1992).
28. M. Landy and A. Freiberger, *J. Colloid Interface Sci.* **25**, 231 (1967).
29. V. F. Petrenko, *J. Phys. Chem. B* **101**, 6276 (1997).
30. I. A. Ryzhkin and V. F. Petrenko, *J. Phys. Chem. B* **101**, 6267 (1997).
31. V. F. Petrenko and I. A. Ryzhkin, *J. Phys. Chem. B* **101**, 6285 (1997).
32. L. A. Wilen, J. S. Wettlaufer, M. Elbaum and M. Schick, *Phys. Rev. B: Condens. Matter* **52**, 12426 (1995).
33. V. F. Petrenko and S. Peng, *Can. J. Phys.* **81**, 387 (2003).
34. L. S. Penn and A. Meyerson, Report, SHRP-W/UFR-92-606, Chemical, Engineering Department, Polytechnic University Brooklyn, NY, April (1992).
35. L. Daikhin and V. Tsionsky, *J. Phys.: Condens. Matter* **19**, 376109 (2007).
36. J. G. Dash, H. Fu and J. S. Wettlaufer, *Rep. Prog. Phys.* **58**, 115 (1995).
37. H. H. G. Jellinek, *Can. J. Phys.* **40**, 1294 (1962).
38. N. U. Nakaya and A. Matsumoto, *J. Coll. Sci.* **9**, 41 (1954).
39. V. F. Petrenko, Report, 96-2; U.S. Army Cold Regions Research Thayer School of Engineering and Engineering Laboratory Dartmouth College Hanover, NH, USA, February (1996).
40. V. Tsionsky, E. Alengoz, L. Daikhin, A. Kaverin, D. Zagidulin and E. Gileadi, *Electrochim. Acta* **50**, 4212 (2005).
41. V. Tsionsky, D. Zagidulin and E. Gileadi, *J. Phys. Chem. B* **106**, 13089 (2002).
42. W. A. Weyl, *J. Coll. Sci.* **6**, 369 (1951).
43. N. H. Fletcher, in: *Physics and Chemistry of Ice*, E. Whaley *et al.* (Eds), Roy. Soc., Ottawa (1973).
44. I. A. Ryzhkin and V. F. Petrenko, *Phys. Rev. B: Condens. Matter* **6501**, 012205 (2002).
45. B. F. Henson and J. M. Robinson, *Phys. Rev. Lett.* **92**, 246107 (2004).
46. V. F. Petrenko and S. Qi, *J. Appl. Phys.* **86**, 5450 (1999).
47. V. F. Petrenko, US 6,427,946 (2002).
48. V. F. Petrenko, US 6,576,115 (2003).
49. V. F. Petrenko and C. Sullivan, US 6,723,971 (2004).
50. J. Druez, C. L. Phan, J. L. Laforte and D. D. Nguyen, *Trans. Can. Soc. Mech. Eng.* **5**, 215 (1978).
51. R. Roe, Report, NASA Engineering and Safety Center, June 29 (2005).

52. D. N. Anderson and A. D. Reich, in: *Proc. of the 35th Aerospace Sciences Meeting & Exhibit*, Reno, NV, USA, January 6–10 (1997).
53. Anon., Report, EM 1110-2-1612; Department of the Army, U.S. Army Corps of Engineers Washington DC, USA, April 30 (1999).
54. D. Hacker, B. White and R. Ferrill, in: *Proc of the ICE 2000, 78th Annual Meeting of the International Coatings Exposition*, Chicago, IL, USA, October 18–20 (2000).
55. V. A. Igoshin and A. G. Berdnikov, *Sov. J. Fric. Wear* (English translation of Trenie i Iznos) **10**, 83 (1989).
56. H. H. G. Jellinek, H. Kachi, S. Kittaka, M. Lee and R. Yokota, *Coll. Polym. Sci.* **256**, 544 (1978).
57. P. Kumar, P. Brisson, G. Weinwurm and J. Clark, *ESA Bulletin* **99** (1999).
58. T. Laakso, H. Holttinen, G. Ronsten, L. Tallhaug, R. Horbaty, I. Baring-Gould, A. Lacroix, E. Peltola and B. Tammelin, Report, Exhibit MH/NCN 1031 section e (2003).
59. A. Lacroix and J. F. Manwell, Report, Exhibit MH/NCN 1031 section b; University of Massachusetts at Amherst, June 2000 (2000).
60. C. Laforte, J. C. Carriere and J. L. Laforte, in: *Proc of the 10th International Workshop on Atmospheric Icing of Structures*, Brno, Czech Republic, June 17–20 (2002).
61. J. F. Maissan, in: *Proc. of the Circumpolar Climate Change Summit and Exposition*, Whitehorse, Yukon, Canada, March 19–21 (2001).
62. A. Reich, in: *Proc. of the AIAA, 32nd Aerospace Sciences Meeting and Exhibit*, Reno, NV, USA, 10–13 January (1994).
63. J. R. Smith and N. N. Garti, US 6,084,020 (2000).
64. L. O. Anderson, C. G. Golander and S. Persson, *J. Adhesion Sci. Technol.* **8**, 117 (1994).
65. www.wearlon.com
66. L. Gastonguay and G. Y. Champagne, in: *Proc. of the 7th International Workshop on Atmospheric Icing of Structures*, Chicoutimi (QC), Canada, June (1996).
67. Anon., Report, Commissariat à l'Energie Atomique (CEA) France, March (2002).
68. B. Somlo and V. Gupta, *Mech. Mater.* **33**, 471 (2001).
69. M. Kemell, E. Färm, E. Santala, M. Ritala and M. Leskelä, in: *Proc. of the TNT 2005 "Trends in Nanotechnology"*, Oviedo, Spain, 29 August–02 September (2005).
70. S. A. Kulinich and M. Farzaneh, *Appl. Surf. Sci.* **230**, 232 (2004).
71. S. A. Kulinich and M. Farzaneh, *Vacuum* **79**, 255 (2005).
72. H. Ji, A. Cote, D. Koshel, B. Terreault, G. Abel, P. Ducharme, G. Ross, S. Savoie and M. Gagne, *Thin Solid Films* **405**, 104 (2002).
73. G. Cicala, A. Milella, F. Palumbo, P. Favia and R. d'Agostino, *Diamond Relat. Mater.* **12**, 2020 (2003).
74. M. Kiuru, *Thesis*, Experimental studies on diamond-like carbon and novel diamond-like carbon — polymer-hybrid coatings, University of Helsinki, Finland (2004).
75. D. Koshel, H. Ji, B. Terreault, A. Cote, G. G. Ross, G. Abel and M. Bolduc, *Surf. Coat. Technol.* **173**, 161 (2003).
76. I. Woodward, W. C. E. Schofield, V. Roucoules and J. P. S. Badyal, *Langmuir* **19**, 3432 (2003).
77. H. Murase, K. Nanishi, H. Kogure, T. Fujibayashi, K. Tamura and N. Haruta, *J. Appl. Polym. Sci.* **54**, 2051 (1994).
78. H. Murase and T. Fujibayashi, *Prog. Org. Coat.* **31**, 97 (1997).
79. N. R. Byrd, US 6,797,795 (2004).
80. S. Mizuno, C. Nishi, Y. Tsukamoto, M. Fujino, T. Yanagawa, T. Ota, H. Yonezawa, K. I. Takai and G. Yamauchi, US 6,579,620 (2003).
81. M. Der Ger, K. H. Hou, L. M. Wang and J. H. Bing, *Mater. Chem. Phys.* **77**, 755 (2002).

82. F. Wang, S. Arai and M. Endo, *Mater. Trans.* **45**, 1311 (2004).
83. W. Barthlott and C. Neinhuis, *Ann. Bot.* **79**, 667 (1997).
84. W. Barthlott and C. Neinhuis, *Planta* **202**, 1 (1997).
85. P. Wagner, R. Furstner, W. Barthlott and C. Neinhuis, *J. Exp. Bot.* **54**, 1295 (2003).
86. Q. Cong, G. Chen, Y. Fang and L. Ren, *J. Bionics Eng.* **1**, 249 (2004).
87. U. Mock, R. Forster, W. Menz and J. Ruhe, *J. Phys.: Condens. Matter* **17**, S639 (2005).
88. A. R. Parker and C. R. Lawrence, *Nature* **414**, 33 (2001).
89. A. Nakajima, K. Hashimoto and T. Watanabe, *Monatshefte fur Chemie* **132**, 31 (2001).
90. X. Wu and G. Shi, *Nanotechnology* **16**, 2056 (2005).
91. T. Soeno, K. Inokuchi and S. Shiratori, *Appl. Surf. Sci.* **237**, 543 (2004).
92. N. Saleema and M. Farzaneh, *Appl. Surf. Sci.* **254**, 2690 (2008).
93. J. Y. Shiu, C. W. Kuo, P. Chen and C. Y. Mou, *Chem. Mater.* **16**, 561 (2004).
94. H. Yan, K. Kurogi, H. Mayama and K. Tsujii, *Angew. Chem. Int. Ed.* **44**, 3453 (2005).
95. Z. Zhang, L. Qu and G. Shi, *J. Mater. Chem.* **13**, 2858 (2003).
96. K. K. S. Lau, J. Bico, K. B. K. Teo, M. Chhowalla, G. A. J. Amaratunga, W. I. Milne, G. H. McKinley and K. K. Gleason, *Nanoletters* **3**, 1701 (2003).
97. J. Zhang, J. Li and Y. Han, *Macromol. Rapid Com.* **25**, 1105 (2004).
98. L. Feng, Y. Song, J. Zhai, B. Liu, J. Xu, L. Jiang and D. Zhu, *Angew. Chem. Int. Ed.* **42**, 800 (2003).
99. M. Ma, Y. Mao, M. Gupta, K. K. Gleason and G. C. Rutledge, *Macromol.* **38**, 9742 (2005).
100. K. Acatay, E. Simsek, C. Ow-Yang and Y. Z. Menceloglu, *Angew. Chem. Int. Ed.* **43**, 5210 (2004).
101. R. Menini and M. Farzaneh, *Polym. Int.* **57**, 77 (2008).
102. H. Saito, K. I. Takai, H. Takazawa and G. Yamauchi, *Mater. Sci. Res. Int.* **3**, 216 (1997).
103. H. Saito, K. I. Takai, H. Takazawa, G. Yamauchi and G. Zairyo, *J. Soc. Mater. Sci. Jpn* **46**, 551 (1997).
104. H. Saito, K. Takai and G. Yamauchi, *NTT R and D* **48**, 337 (1999).
105. H. Saito, K. Takai and G. Yamauchi, *Surf. Coat. Int.* **4**, 168 (1997).
106. H. Saito, K. I. Takai and G. Yamauchi, *Mater. Sci. Res. Int.* **3**, 185 (1997).
107. A. Safaee, D. K. Sarkar and M. Farzaneh, *Appl. Surf. Sci.* **254**, 2493 (2008).
108. N. Saleema, M. Farzaneh and R. Paytner, in: *Proc. of the 6th Symposium on Functional Coating and Surface Engineering (FCSE)*, Montreal, QC, Canada (2008).
109. D. K. Sarkar and M. Farzaneh, *Appl. Surf. Sci.* **254**, 3758 (2008).
110. B. He, N. A. Patankar and J. Lee, *Langmuir* **19**, 4999 (2003).